Cytochrome a_3 Hemepocket Relaxation Subsequent to Ligand Photolysis from Cytochrome Oxidase

E. W. Findsen,[†] J. Centeno,[‡] G. T. Babcock,[‡] and M. R. Ondrias*[†]

Contribution from the Department of Chemistry, University of New Mexico, Albuquerque, New Mexico 87131, and Department of Chemistry, Michigan State University, East Lansing, Michigan 48824. *Received December 15, 1986*

Abstract: Time-resolved resonance Raman spectroscopy has been employed to monitor the full time course of cytochrome a_3 hemepocket relaxation subsequent to carbon monoxide photolysis from fully reduced cytochrome oxidase. This study has demonstrated that the cytochrome a_3 hemepocket undergoes significant reorganization in response to ligand photolysis from heme a_3. It is the first of its kind to trace the evolution of such hemepocket dynamics in a redox-active catalytic protein. Some similarities in the photolytic species of cytochrome a_3 and hemoglobin were apparent, but the general response to ligand photolysis of the proteins was quite distinct. The absence of any distinct bands assignable to the CO ligated heme a_3 in the initial (10 ns) transient spectra contrasts with the behavior of hemoglobin under similar conditions. Heme a_3–carbon monoxide geminate recombination is evidently slow on a 10-ns time scale or nonexistent. Differences in the correlation between Fe–His bond strength and porphyrin π^* electron density and the kinetics of both proximal hemepocket relaxation and ligand rebinding were also apparent. Collectively, they suggest significant generic alterations in the nature of the heme–protein dynamics between hemoglobins and cytochrome oxidase resulting from specific structural differences within their respective hemepockets.

During the past decade an increasing number of experimental and theoretical studies have revealed that the dynamic interactions between protein active sites and their local environment can play significant roles in the functional behavior of these complex systems (for general reference, see ref 1–4). The dynamics of heme-containing proteins, in particular, have been studied by a variety of experimental techniques. Most of these probed either the fluctuational dynamics of the protein about equilibrium configurations or utilized cryogenic techniques to trap intermediate kinetic species. Direct, room temperature investigation of the molecular dynamics involved in the kinetics of functional processes (i.e., ligand binding, electron transfer, and catalysis) has been largely confined to transient absorption studies.

Recently time-resolved resonance Raman spectroscopy, in the ps to μs time scale, has been applied to hemeproteins.[5-22] This technique offers a variety of advantages over time-resolved absorption spectroscopy. Chief among these is the much larger information content of vibrational spectra. This is especially true for enzymes containing heme active sites owing to the very large data base available that characterizes the structural bases for the resonance Raman properties of equilibrium hemeproteins and model complexes. Heme resonance Raman spectra can now be unambiguously interpreted to yield specific information concerning heme geometric and electronic properties and heme–axial ligand bonding interactions. Changes in these molecular parameters at the protein active site can then be used to infer the extent and nature of heme–protein interactions during various functional processes. Moreover, these observations may be made at room temperature under physiologically relevant solution conditions.

The proteins most extensively investigated by transient resonance Raman spectroscopy to date are hemoglobins (Hb) and myoglobins (Mb). Several laboratories have probed the transient heme species generated subsequent to ligand photolysis from Hb and Mb by using single-pulse techniques that yield data from a single time point on the ps or the ns time scale.[5-15] Those studies demonstrated that, in hemoglobin, the heme–protein interactions subsequent to photolysis differ significantly from those of the equilibrium protein. The photolytic transient species, when compared to the equilibrium unligated species, exhibit changes in heme core size, heme peripheral environment, and the Fe–proximal histidine bond strength. The behavior of the Fe–His bond can be further analyzed to infer relaxation processes within the proximal hemepocket.

Interestingly, the transient differences observed on a nanosecond time scale in tetrameric hemoglobins are absent in the noncooperative myoglobin monomer. In an elegant series of experiments, Scott and Friedman[5] traced the time evolution of the Fe–His bond strength after photolysis by using a two-pulse, pump-probe technique. They found that not only the initial transient geometry of the proximal hemepocket but also its relaxation lifetime were highly dependent upon parameters that also control ligand affinity. These include protein quaternary structure and variations in protein tertiary structure resulting from species or solution differences (e.g., pH). These data, in turn, can be correlated with various theoretical predictions concerning the motions of the protein "allosteric core" and transition-state arguments for ligand-binding mechanisms.

*To whom correspondence should be addressed.
[†]University of New Mexico.
[‡]Michigan State University.

(1) Karplus, M.; McCammon, J. A. *CRC Crit. Rev. Biochem.* **1981**, *9*, 293.
(2) Gurd, F. R. N.; Rothgeb, T. M. *Adv. Protein Chem.* **1979**, *33*, 74.
(3) Debrunner, P. G.; Frauenfelder, H. *Ann. Rev. Phys. Chem.* **1982**, *33*, 283.
(4) Friedman, J. M.; Rousseau, D. L.; Ondrias, M. R. *Ann. Rev. Phys. Chem.* **1982**, *33*, 471.
(5) Scott, T. W.; Friedman, J. M. *J. Am. Chem. Soc.* **1984**, *106*, 5677.
(6) Friedman, J. M.; Stepnoski, R. A.; Stavola, M.; Ondrias, M. R.; Cone, R. *Biochemistry* **1982**, *21*, 2022.
(7) Woodruff, W. H.; Farquhausen, S. *Science* **1978**, *201*, 183.
(8) Findsen, E. W.; Friedman, J. M.; Ondrias, M. R.; Simon, S. R. *Science* **1985**, *228*, 661.
(9) Findsen, E. W.; Friedman, J. M.; Scott, T. W.; Chance, M. R.; Ondrias, M. R. *J. Am. Chem. Soc.* **1985**, *107*, 3355.
(10) Friedman, J. M.; Rousseau, D. L.; Ondrias, M. R.; Stepnoski, R. A. *Science* **1982**, *218*, 1244.
(11) Dasgupta, S.; Spiro, T. G.; Johnson, C. K.; Dalikas, G. A.; Hochstrasser, R. M. *Biochemistry* **1985**, *24*, 5295.
(12) Terner, J.; Stong, J. D.; Spiro, T. G.; Nagumo, M.; Nicol, M. F.; El-Sayed, M. A. *Proc. Natl. Acad. Sci. U.S.A.* **1981**, *78*, 1313.
(13) Ondrias, M. R.; Friedman, J. M.; Rousseau, D. L. *Science* **1983**, *220*, 614.
(14) Irwin, M. J.; Atkinsen, G. H. *Nature (London)* **1981**, *293*, 37.
(15) Findsen, E. W.; Alston, K.; Shelnutt, J. W.; Ondrias, M. R. *J. Am. Chem. Soc.* **1986**, *108*, 4009.
(16) Findsen, E. W.; Ondrias, M. R. *J. Am. Chem. Soc.* **1984**, *106*, 5736.
(17) Smulevich, G.; Spiro, T. G. *Biochim. Biophys. Acta* **1985**, *830*, 80.
(18) Alden, R. G.; Ondrias, M. R. *J. Biol. Chem.* **1985**, *260*, 2194.
(19) Babcock, G. T.; Jean, J. M.; Johnston, L. N.; Woodruff, W. H.; Palmer, G. *J. Am. Chem. Soc.* **1984**, *106*, 8305.
(20) Babcock, G. T.; Jean, J. M.; Johnston, L. N.; Woodruff, W. H.; Palmer G. *J. Inorg. Biochem.* **1985**, *23*, 243.
(21) Ogura, T.; Yoshikawa, S.; Kitagawa, T. *Biochem. Biophys. Acta* **1985**, *832*, 220.
(22) Gaul, D. F.; Ondrias, M. R.; Findsen, E. W.; Palmer, G.; Olson, J. S.; Davidson, M. W.; Knaff, D. B. *J. Biol. Chem.* **1987**, *262*, 1144.

0002-7863/87/1509-5367$01.50/0

Recently, several laboratories have undertaken the investigation of heme photolytic transients in various hemeproteins. Peroxidases, bacterial ligand binding proteins, and mammalian cytochrome oxidase have been examined.[16-22] Initial, single-pulse studies yielding 10-ns transient species have revealed a wide variation in the types and magnitudes of the heme–protein interactions subsequent to carbon monoxide photolysis in the systems examined. These range from the complete absence of transient species in a monomeric oxygen-binding protein isolated from Chromatium vinosum[22] to the extensive transient changes exhibited by cytochrome oxidase.[16]

This report presents the results of the first extended time-resolution, two-pulse transient Raman investigation of the evolution of photolytic heme transient species in a redox active protein. Cytochrome oxidase is an inherently more complex system than hemoglobin. It possesses catalytic, electron transfer, and proton pumping functions as well as ligand binding properties. Moreover, it contains four redox centers that actively participate in the enzyme's reduction of dioxygen to water. These consist of two heme *a* moieties and two copper-containing sites which apparently function in a pairwise (one heme, one copper) fashion. The ligand binding site of the protein, designated cytochrome a_3, is composed of a magnetically coupled heme a_3–Cu_B pair. The spectroscopic characterization of the local equilibrium structure about the redox centers of cytochrome oxidase has recently been the focus of extensive investigations. However, the molecular mechanisms by which this protein carries out its various physiological functions remain unclear. Cryogenic studies of catalytic intermediates of dioxygen reduction and ligand binding rates suggest that conformational dynamics at the redox sites may play roles in the functioning of this complex system.[23-27] Initial transient Raman studies have confirmed that structural relaxation at the heme a_3 site occurs subsequent to CO photolysis[16] and have provided evidence for the formation of oxy intermediates during O_2 reduction.[19,20] The present work extends these observations by tracing the time evolution of hemepocket relaxation and ligand rebinding at cytochrome a_3 in the fully reduced enzyme.

Materials and Methods

Bovine cytochrome oxidase was prepared by using a modified Hartzell–Bienert preparation.[28] Samples of fully reduced cytochrome oxidase were prepared in either of two ways. In the first, the sample was degassed by 6–8 cycles of alternating vacuum and oxygen-free N_2 gas. Sodium dithonite (J. T. Baker Chemical Co.) was added under positive N_2 pressure to produce the reduced species. The sample was then cycled 4–5 times between vacuum and carbon monoxide atmospheres with the final pressure of CO over the sample between 600 and 700 mm of Hg. The CO was scrubbed by passing it through a solution of 2 M KOH before use. The second method was identical with the above procedure except that CO was used during the entire procedure. No difference between the samples produced by the two methods was observed. All samples were prepared in 50 mM HEPES (*N*-(2-hydroxyethyl)-piperazine-*N*-2-ethanesulfonic acid (Calbiochem—Behring) and either 0.5% Brij (poly(oxyethylene) 23-lauryl ether) (Sigma Chemical) or dodecyl-β-D-maltoside (Calbiochem—Behring). The final pH of the samples was found to be between 7.2 and 7.4 in all cases. Samples were contained in an anerobic rectangular cell constructed from quartz tubing with a cross section of 3 × 5 mm. Sample integrity was monitored by absorption spectroscopy before and immediately after each Raman experiment. No sample degradation was observed in any sample during the course of these experiments as determined by optical absorption assays.

The one- and two-pulse time-resolved Raman spectrometers have been described in detail elsewhere.[29] Briefly, The two-pulse system consists of two pulsed lasers, both with nominal pulse widths of ≈10 ns, a digital delay generator (Cal Avionics, 113BR) which controls the triggering of the lasers, a PAR/EG&G Model 162 boxcar with 165 plugin, and a SPEX Ind. 1403 scanning monochromator with a SPEX Ind. Datamate DM-1 which stores data during acquisition and controls the monochromator. The scattered radiation was collected by using a backscattering geometry and focused into the monochromator through a polarization scrambler. A cooled photomultiplier (Hamamatsu RP-928) was used for detection.

The photolyzed transient was generated by using the second harmonic output (532 nm) of a Quanta-Ray DCR-II laser system. The pump laser energy incident on the sample was kept below ≈5.0 mJ/pulse by use of neutral density filters. The probe laser consisted of a Molectron UV-24 N_2 laser which pumped a Molectron DL-24 dyelaser equipped with a flowing dye cell system. The laser frequency used to probe the transient was 440 nm (Coumarin 440 dye (Exciton)). The probe power incident on the sample was between 0.3 and 0.5 mJ/pulse. The output of both lasers was imaged onto the sample with cylindrical lenses. The laser repetition rate in all experiments was ~10 Hz. The delay time between the pump and probe pulses was controlled by using a digital delay generator. This delay was continuously monitored with a photodiode to collect scattered laser light and a Tektronix 4540 oscilloscope to observe the delay.

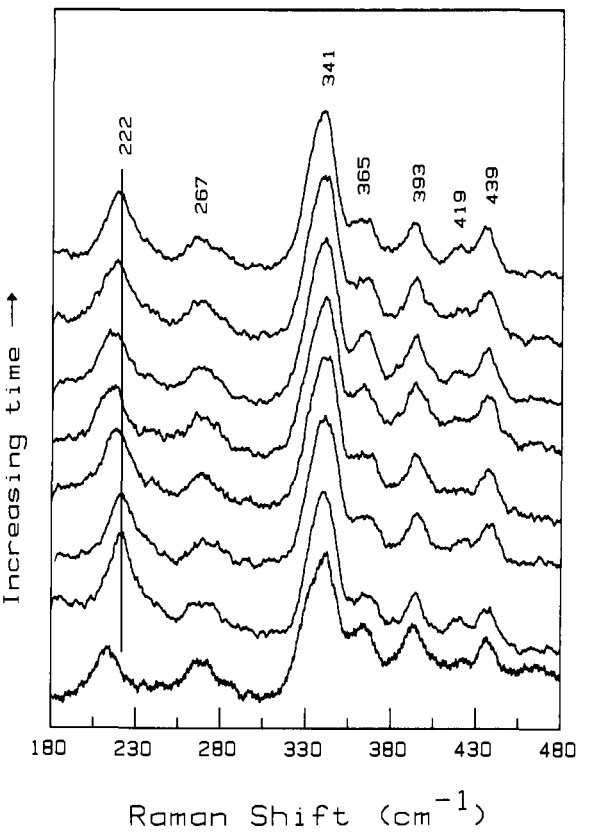

Figure 1. Low-frequency time-resolved spectra of cytochrome oxidase subsequent to CO photolysis in ascending order: (a) equilibrium reduced oxidase, (b) 10 ns, (c) 125 ns, (d) 1 μs, (e) 150 μs, (f) 750 μs, (g) 1 ms, (h) 5 ms. Obtained with 532 nm and 440 nm pump and probe beams respectively as described in the text. Spectra are the unsmoothed sums of 3–5 scans at 10 cm^{-1}/min. Spectral band-pass was ≤7 cm^{-1} in all cases.

Results

Representative resonance Raman spectra of cytochrome oxidase obtained at various times subsequent to carbon monoxide photolysis from cytochrome a_3 in the low- and high-frequency regions are shown in Figures 1 and 2, respectively (see ref 30 for a summary of heme vibrational assignments for cytochrome oxidase). At the laser powers and protein concentrations used, the sample within the illuminated volume was completely photolyzed by the initial pump pulse. No dependence upon laser repetition rate (5–20 Hz) or protein concentration was evident in the ambient pressure

(23) Clore, G. M.; Chance, E. M. *Biochem. J.* **1978**, *173*, 811.
(24) Sharrock, M.; Yonetani, T. *Biochim. Biophys. Acta* **1977**, *462*, 718.
(25) Fiamingo, F. G.; Altschuld, R. A.; Moh, P. P.; Alben, J. O. *J. Biol. Chem.* **1982**, *257*, 1639.
(26) Blair, D. F.; Witt, S. N.; Chan, S. I. *J. Am. Chem. Soc.* **1985**, *107*, 7389.
(27) Witt, S. N.; Blair, D.; Chan, S. I. *J. Biol. Chem.* **1986**, *261*, 8104.
(28) Babcock, G. T.; Vickery, L. E.; Palmer, G. *J. Biol. Chem.* **1976**, *251*, 7904.
(29) Findsen, E. W. Ph.D. Dissertation, University of New Mexico, 1986.
(30) See: Babcock, G. T. In *Biological Applications of Raman Scattering*; Spiro, T. G., Ed., in press and references therein.

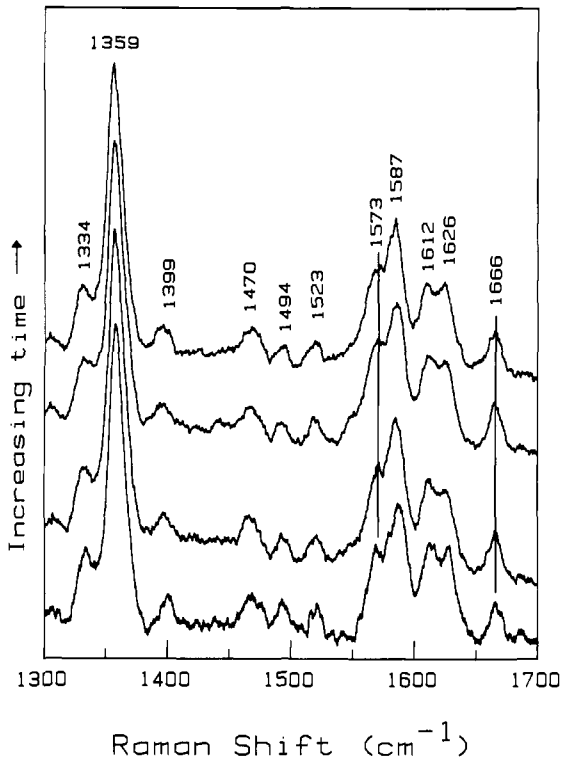

Figure 2. High-frequency time-resolved spectra of cytochrome oxidase subsequent to CO photolysis in ascending order: (a) equilibrium reduced oxidase, (b) 10 ns, (c) 1 μs, (d) 750 μs. Conditions were the same as for Figure 1.

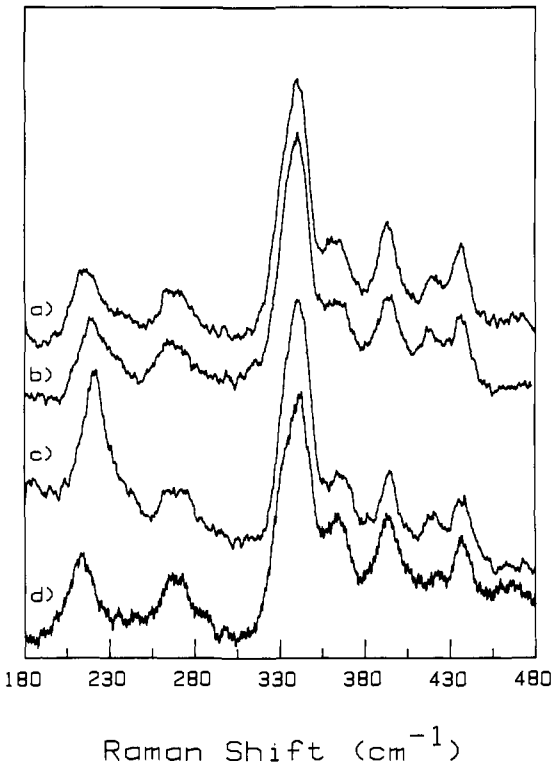

Figure 3. Comparison of 10-ns photolytic transients of cytochrome oxidase: (a) 100 Torr of CO, 19 Hz laser rep. rate, (b) 100 Torr CO, 5 Hz laser rep. rate, (c) ~800 Torr CO, 10 Hz laser rep. rate, (d) equilibrium reduced oxidase. All other conditions were the same as for Figure 1.

spectra. Samples prepared in either 0.5% Brij or 0.5% lauryl maltoside detergents displayed essentially identical behavior.

Spectra of oxidase photolytic transients obtained at early times (<200 ns) subsequent to CO photolysis display the following characteristics relative to spectra of equilibrium fully-reduced oxidase: (1) the mode at ~214 cm^{-1} which has been previously assigned as the heme a_3 Fe–His stretching mode shifts to higher frequency, (2) heme a_3 modes at ~365 and ~420 cm^{-1} display intensity and/or position changes, (3) the heme a_3 core-size sensitive band, ν_2, at ~1570 cm^{-1} appears to shift to higher frequency, and (4) identical spectra of the 10-ns heme a_3 transient were obtained with either Soret (440 nm) or visible (532 nm) band excitation to produce CO photolysis. This behavior is analogous to that observed in photolytic transients of HbCO. Interestingly, neither the heme a_3 formyl stretching mode (~1665 cm^{-1}) nor the porphyrin π^* electron density sensitive mode, ν_4 (~1359 cm^{-1}), display frequency shifts in the photolytic transients relative to the equilibrium species. The behavior of ν_4 in the heme a_3 transient is in contrast to the correlated shifts in ν_4 and ν_{Fe-His} exhibited by Hb photolytic transients.

The sensitivity of the initial (10 ns) heme a_3 transient spectra to CO pressure (50–700 Torr) was also examined. Variations in CO pressure above the sample were found to induce apparent differences in the spectrum of the heme a_3 photolytic transient (see Figure 3). Shifts in ν_{Fe-His} and ν_2 relative to the equilibrium species are not nearly as pronounced at lower CO pressure. At 200 Torr of CO, the Fe–His mode of the heme a_3 10-ns transient occurs at ~218 cm^{-1} while the position of the ν_2 is indistinguishable from that of fully reduced equilibrium oxidase. This phenomenon was strongly dependent upon laser repetition rate and almost surely results from the lack of complete CO rebinding between laser pulses by the sample at low CO concentrations. For the high-pressure samples (~1 atm of CO) the pseudo-first-order rate constant for CO rebinding, K_{on}[CO], is $\geq 10^2$ (using $K_{on} \simeq 10^5$ M^{-1} s^{-1} and [CO] at 1 atm $\approx 10^{-3}$ M), producing a rebinding half-life that is short compared to the ~100-ms period between laser pulses. As the CO concentration is reduced, the rebinding half-life begins to approach 100 ms and the laser pulses interogate a mixed population of religated and unligated (and now fully relaxed) equilibrium oxidase molecules, producing spectra of mixtures of the two species (i.e., more similar to the equilibrium unligated species).

The two-pulse protocol was used to probe both the relaxation of the heme a_3 pocket to its equilibrium unligated configuration and the rebinding of CO to the photolyzed heme a_3 site. The latter phenomenon manifests itself as the growth of an Fe–His peak (shoulder) at ~222 cm^{-1} at longer (>500 μs) time intervals. This results from the photolysis of ligated sites by the probe beam, producing a 10-ns transient spectrum. Since we are photolyzing virtually all of the heme a_3·CO sites with the pump beam, the appearance of a ν_{Fe-His} peak at ~222 cm^{-1} signals the onset of ligand rebinding to the previously photolyzed sites. Figures 1 and 2 depict the time evolution of the resonance Raman spectra of photolyzed oxidase on a ns to ms time scale. Both cytochrome a_3 hemepocket evolution and the onset of ligand rebinding are evident in the low-frequency spectra.

Figure 4 graphically depicts the relaxation of the Fe–His mode to its equilibrium position (~214 cm^{-1}) following CO photolysis from heme a_3. The sharp rise in frequency of this mode in the 1–10-ms range reflects the rebinding of CO to heme a_3 and the subsequent photolysis of the rebound heme a_3·CO sites. The other spectral differences noted above between the transient and equilibrium heme a_3 species decay on time scales qualitatively similar to that observed for ν_{Fe-His}.

Examination of Figure 4 reveals several salient aspects of the relaxation of the heme a_3 pocket: (1) the rate of relaxation falls within the range exhibited as a function of pH by Hb,[5] (2) relaxation is bi-phasic with little or no relaxation of the Fe–His frequency occurring in the first 200 ns subsequent to ligand photolysis, and (3) ligand rebinding to heme a_3 occurs on a dramatically longer time scale (at room temperature) than ligand rebinding in Hb.

Discussion

Nature of the Heme a_3 Photolytic Transient. The transient resonance Raman spectra of heme a_3 generated within 10 ns of ligand photolysis arise from unstable intermediates that result from

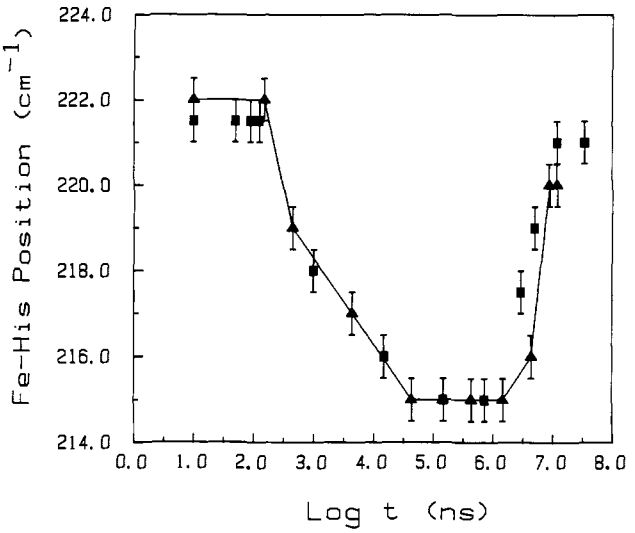

Figure 4. Plot of Fe–His mode position vs. log time subsequent to CO photolysis. Samples were prepared in either Brij (■) or maltoside (△) detergents as described in the text. The solid line is drawn only to aid the eye.

the large disparity in the relaxation rate of the heme relative to its surrounding protein matrix. These phenomena span a time scale from subpicoseconds to milliseconds. Initial excitation of heme π–π^* transitions has been postulated to decay into either of two dissociative transitions involving heme–CO charge transfer.[31] Transient absorption studies place these events and the iron spin-state change which accompanies dissociation in the subpicosecond time scale.[41] Relaxation of the heme geometry then occurs in response to these electronic changes. The major readjustment in heme geometry is the expansion of the porphyrin core size and the concomitant motion of the heme iron to an out-of-plane position characteristic of the unligated species. These events have been documented by transient Raman studies to occur in <50 ps after CO photolysis from Mb and Hb.[4-15] The electronic and geometric alterations occurring in the first ns after photolysis at the heme may create a metastable situation within the hemepocket. If the protein matrix surrounding the heme active site undergoes significant reorganization upon ligand binding then the heme–protein interactions immediately subsequent to ligand photolysis will be distinct from, but evolve to, those of the equilibrium unligated hemepocket. It is this transient hemepocket geometry that is probed by resonance Raman studies in the ns to ms time range. Direct modulation of heme reactivity by the protein matrix has been suggested on both theoretical and experimental grounds to play a pivotal role in hemeprotein functional mechanisms.[1-5]

The metastable geometry of the a_3 hemepocket that occurs within 10 ns of CO photolysis (see Figure 1) clearly results in a heme a_3 resonance Raman spectrum distinct from that of the equilibrium unligated protein. This species most probably represents the initial geometry of the heme pocket subsequent to the direct electronic and geometric relaxation of the heme itself. Previous ps time-resolved studies of Hb have established that the altered Fe–His bond strength observed in the transient species (vide infra) and its dependence upon solution conditions are the same at 30 ps and 10 ns subsequent to photolysis.[8] Picosecond and nanosecond transient Raman studies of Mb·CO photolysis reveal no transient Fe–His geometry at room temperature.[9] Only direct relaxation of the heme can be observed to occur in <1 ns.[11]

The chief perturbation in heme–protein interactions occurs in the binding of the histidine to the heme iron. The mode at ~214 cm^{-1} in reduced unligated cytochrome oxidase has been assigned as the a_3 Fe–His stretching mode.[30] The increased frequency of this mode in the photolytic transient is analogous to that observed in hemoglobins and is indicative of a strengthened bond. For hemoglobins, this effect has been postulated to result from a more upright histidine tilt angle (in its own plane) relative to the heme plane in the hemoglobin transients. Our data indicate a similar scenario is operative for the heme a_3 site. Other degrees of freedom such as histidine rotation relative to the heme or variation in hydrogen bonding of the proximal histidine may play roles in the transient behavior of the a_3 hemepocket. Moreover, the biphasic behavior of the cytochrome a_3 proximal pocket relaxation suggests that the forces responsible for hemepocket reorganization subsequent to photolysis are not located in the proximal pocket of the equilibrium ligated species as considered in more detail below.

The other low-frequency spectral signatures of the heme a_3 photolytic transient parallel those of Hb transients. The intensity and frequency variations of the ~365 and ~420 cm^{-1} heme a_3 modes may be generically similar to variations observed in the ~345 and ~420-cm^{-1} modes of Hb.[5,13] These modes have been assigned as in-plane bending motions of heme peripheral substituents.[30] Their variability between transient and equilibrium species may be indicative of an altered heme a_3 rotational position within the hemepocket.

While a fairly strong analogy can be drawn between the low-frequency spectra of Hb and heme a_3 photolytic transients, the high-frequency spectra reveal quite different behavior. The photolytic transients of a variety of hemoglobins have been studied by time-resolved Raman spectroscopy and, with the exception of noncooperative monomeric hemoglobins, each displays shifts in ν_4 (~1357 cm^{-1}) of the transient species to lower frequency (by 1 to 4 cm^{-1}) relative to the equilibrium species. Quantification of small frequency shifts in ν_4 for heme a_3 transients is complicated by the substantial contribution from heme a^{2+} scattering (presumed to be unaffected by CO photolysis from cytochrome a_3 at short times) to the band at 1359 cm^{-1}. Nonetheless within our detection limits (±1 cm^{-1}), no such behavior is evident in our spectra of cytochrome oxidase. This mode is quite sensitive to the electron density of the iron with lower frequency indicating increased density. The magnitudes of the ν_4 frequency shifts in photolytic transients of various hemoglobins has recently been correlated to their Hill coefficients.[33] In equilibrium human hemoglobins an inverse relationship exists between the positions of Fe–His and ν_4.[34] These observations suggest an intimate connection between the heme electronic properties and the local hemepocket geometry. This relationship is apparently absent in cytochrome a_3. Thus the electronic ramifications of the transient hemepocket geometry seem to be radically different for these two classes of proteins.

The absence of any distinct band assignable to the CO liganded heme a_3 site in transient spectra generated with moderate laser power (≤0.5 mJ/pulse) contrasts with the behavior of HbCO under similar conditions, where the rapid geminate recombination of CO produces a significant amount of religated HbCO within 10 ns of photolysis. The heme–carbon monoxide geminate recombination rate in cytochrome oxidase is evidently slow on a 10-ns time scale.

No variability was detected in the heme a_3 10-ns transient species when 440- or 532-nm light was used to initiate photolysis. Thus, the initial geometric disposition of the hemepocket is independent of whether Soret or visible π–π^* transitions are used to trigger ligand photolysis. This is not surprising in view of the time scale anticipated for decay of the π–π^* state (<10 ps).[35]

(31) Waleh, A.; Loew, G. H. *J. Am. Chem. Soc.* **1982**, *104*, 2346.
(32) Argade, P. V.; Ching, Y. C.; Rousseau, D. L. *Science* **1984**, *225*, 329.
(33) Carson, D. S.; Wells, C. A.; Findsen, E. W.; Friedman, J. M.; Ondrias, M. R. *J. Biol. Chem.* **1987**, *262*, 3044.
(34) Ondrias, M. R.; Rousseau, D. L.; Shelnutt, J. A.; Simon, S. R. *Biochemistry* **1982**, *21*, 3428.
(35) Dixon, D. W.; Kirmaier, C.; Holten, D. J. *J. Am. Chem. Soc.* **1985**, *107*, 808.
(36) Gelin, B. R.; Lee, A. W.-M.; Karplus, M. *J. Mol. Biol.* **1983**, *171*, 489.
(37) Gibson, W.; Greenwood, C. *Biochem. J.* **1963**, 541.
(38) Szabo, A. *Proc. Natl. Acad. Sci. U.S.A.* **1978**, *75*, 2108.
(39) Ching, Y. C.; Argade, P.; Rousseau, D. *Biochemistry* **1985**, *24*, 4938.
(40) Gibson, Q. H.; Greenwood, C. *Biochem. J.* **1963**, *86*, 541.
(41) Martin, J. L.; Migus, A.; Poyart, C.; Lecarpentier, Y.; Astier, R.; Antonetti, A. *Proc. Natl. Acad. Sci. U.S.A.* **1983**, *80*, 173.

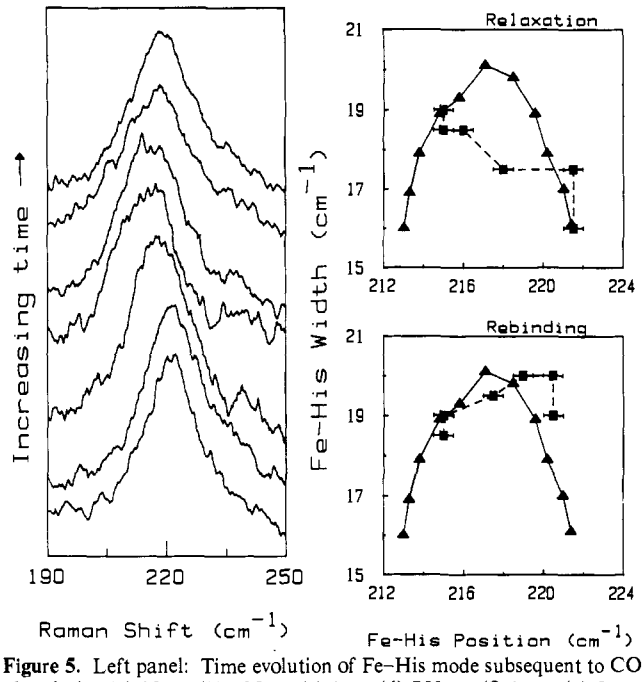

Figure 5. Left panel: Time evolution of Fe–His mode subsequent to CO photolysis: (a) 10 ns, (b) 125 ns, (c) 1 μs, (d) 750 μs, (f) 1 ms, (g) 5 ms, (h) 20 ms in ascending order from the bottom. Right panel: Comparison of line width vs. frequency for (—) two-step model using Gaussian peaks centered at 222 and 213 cm^{-1} with Γ = 16 cm^{-1} and (– – –) experimentally observed behavior for relaxation (upper plot) and rebinding (lower plot) portions of ν_{Fe-His} evolution.

However, molecular orbital calculations[31] indicate at least two photolytic decay pathways exist in protoporphyrins. Both are of d_π, porphyrin $\Pi \rightarrow d_{z^2}$ character. One might anticipate that differences in photolysis pathways would be reflected in the local heme geometry subsequent to photolysis which might, in turn, propagate to the transients observed at 10 ns. The energy levels of the dissociative states have been calculated to be very dependent upon ligand geometry and the extent of ligand–heme π mixing.[31] For the bent CO configuration found in HbCO both dissociative transitions lie below the B and Q bands and are accessible decay pathways from either state. Thus, even on a 30-ps time scale there is no differential effect of B or Q band induced photolysis upon heme photolytic transient spectra for HbCO. A similar situation appears to exist for heme a_3·CO although picosecond experiments are required for a definitive answer.

Cytochrome a_3 Hemepocket Relaxation. The continuous variability of ν_{Fe-His} over a 10 ns–1 ms time scale is the most easily quantified aspect of the hemepocket relaxation and is depicted in Figure 5. This behavior could be the direct result of either the continous evolution of a distribution of Fe–His geometries or the time-dependent conversion of a single species ($\sim$222 cm^{-1}) into the equilibrium geometry with $\nu_{Fe-His} \approx$ 215 cm^{-1}. The evolution of the Fe–His mode in Hb subsequent to CO photolysis has been implicity assumed to result from a continuous distribution rather than from a two-state model.[5] However, the inherent line width of ν_{Fe-His} precludes the direct observation of two distinct Fe–His modes as predicted by the two-state model. This is especially true for hemoglobin which displays an $\sim$20 cm^{-1} line width for ν_{Fe-His}.

To discriminate between these alternative hypothesis, we have modeled the behavior of ν_{Fe-His} predicated upon the two-state scenario. This situation might arise, for example, from a step-function variation in proximal histidine hydrogen bonding between transient and equilibrium species. Figure 5 depicts net response of a ν_{Fe-His} bond composed of varying ratios (10:0 to 0:10) to two modes. The line widths and frequencies used in the calculation are those of the equilibrium reduced and 10-ns photolytic transient species, respectively. It is apparent that this scenario produces a continuous evolution in the net frequency of the band and at no time are two distinct peaks apparent in the spectrum. There is, however, a distinct broadening (by $\sim$25%) in the net line width which reaches a maximum for a 1:1 ratio. As shown in Figure 5, our data do not exhibit the required systematic broadening during the relaxation of the heme pocket (10 ns > Δt > 1 ms). Indeed, except for an initial narrowing in the 10-ns transient (relative to the equilibrium species) the line width of ν_{Fe-His} remains nearly constant as the hemepocket relaxes. The broadening of the Fe–His bond during the 200 ns subsequent to photolysis occurs without an accompanying shift in peak frequency and is indicative of some initial hemepocket relaxation. This might result from an increase in the heterogeneity of the rotational heme–histidine geometry. However, it is apparent that the hemepocket does not interconvert between two discrete geometries (one with ν_{Fe-His} = 214 cm^{-1} and the other with ν_{Fe-His} = 222 cm^{-1}). Rather, the pocket evolves in a viscoelastic manner with a continuum of available geometries. Following the onset of CO rebinding (Δt > 1 ms), however, the line width of ν_{Fe-His} is broadened to 19–20 cm^{-1} (see Figure 5). This is consistent with the fact that there are now two distinct species present, those a_3 sites that have yet to rebind CO and those that have already rebound CO and were subsequently photolyzed by the probe beam.

The evolution of the Fe–His mode most probably arises from fairly large scale motions of the protein proximal pocket which induce the tilt and/or rotation of the histidine in a manner analogous to that postulated for hemoglobins. The time scale for this rearrangement in oxidase is comparable to that of R-state hemoglobin at neutral pH,[5] exhibiting a half-life of $\sim$1 μs. A detailed model for hemepocket relaxation is not possible for oxidase since no crystallographic data of suitable resolution exists. However, dynamics in the μs time range would seem to require either concerted motions of protein helices such as the motion of the "allosteric core" postulated from theoretical modeling of Hb dynamics[36] and/or fairly substantial activation barriers to protein rearrangement. Determination of relaxation rate as a function of temperature may allow for discrimination between these possibilities.

While the time scale and continuous nature of cytochrome a_3 hemepocket relaxation are generally similar to those of Hb, two important distinctions exist in the dynamic behavior of these proteins. First, the relaxation of cytochrome a_3 is clearly biphasic with little or no changes evident in the proximal hemepocket in the first 200 ns after photolysis. Some minor hemepocket evolution occurs during this time and manifests itself in the broadening of ν_{Fe-His}. We speculate that this results from an increase in the rotational heterogeneity of the histidine about the heme normal and is of little energetic importance. In contrast, the evolution of the ν_{Fe-His} frequency in Hb (at pH $\leq$7.5) commences within 50 ns of photolysis. Second, we find no evidence for geminate recombination of CO within a μs of photolysis from cytochrome a_3. This is a marked departure from Hb behavior where geminate CO recombination occurs rapidly ($\tau_{1/2} \sim$ 100 ns) unless the sample is maintained at >30 °C. The ligand rebinding/distal pocket characteristics of cytochrome oxidase are discussed in a later section.

The early time (<200 ns) transient behavior of ν_{Fe-His} suggests that cytochrome a_3 proximal hemepocket finds itself in a metastable geometry subsequent to photolysis. This clearly implies the existence of at least one intermediate conformation that converts to a second species exhibiting the observed decay kinetics (for the frequency of ν_{Fe-His}) to the equilibrium conformation

$$\underset{\nu_{Fe-His}}{a_3 \cdot CO} \xrightarrow{h\nu} \underset{(222\ cm^{-1})}{a_3^*} \xrightarrow{k_1} \underset{(222\ cm^{-1})}{a_3^\dagger} \xrightarrow{k_2} \underset{(214\ cm^{-1})}{a_3}$$

The equivalent ν_{Fe-His} frequencies for a_3^* and $a_3^\dagger$ suggest that the protein forces that ultimately produce an equilibrium Fe–His configuration do not influence the proximal hemepocket at t < 200 ns. The propagation of those forces through the protein to the proximal hemepocket corresponds to the rate constant k_1, above, while k_2 represents the decay kinetics of the hemepocket subsequent to the initial protein reorganization. This behavior contrasts sharply with the postulated mechanism for Hb hemepocket relaxation. For Hb, the process of pulling the iron into

plane upon ligation presumably creates "strain" in the proximal pocket and protein allosteric core by dictating that the histidine assume a more vertical position with respect to the heme (see ref 5 and 10 for a complete discussion). Upon photolysis the iron moves out of plane and the "strain" stored in the proximal pocket is rapidly (<20 ns) manifested as the driving force for the geometric rearrangement of the proximal hemepocket (i.e., $k_1 \gg k_2$ in the above scheme). Thus, the "trigger" for protein rearrangement arises from the motion of the heme iron and the concomitant release of constraints at the heme for a vertical histidine. Cytochrome a_3 proximal hemepocket relaxation subsequent to photolysis apparently is not directly triggered by the heme iron motion. This suggests that the forces acting to reorient the proximal histidine–heme geometry are not resident within the proximal pocket of the ligated protein.

Since ligand binding is a reversible process, the relaxation pathways of heme–protein interactions observed subsequent to photolysis are relevant to the mechanistic function of cytochrome oxidase. A transient Raman study of oxygen binding to cytochrome a_3 by Babcock et al.[19] established that a photolabile species is formed within 10 μs of O_2 binding, but at times greater than 50 μs the cytochrome a_3·O_2 complex becomes resistant to photolysis. Our results indicate that at times >10 μs, one would anticipate that the proximal heme geometry of the complex would be fully relaxed. This supports the inference that the structural determinants for the photolytic behavior of the oxygen complex arise from distal interactions such as the bridging of the O_2 between heme a_3 and Cu_B postulated by Babcock et al.[19]

Ligand Rebinding. Figure 4 shows the kinetics of CO rebinding to the photolyzed heme a_3 site. The onset of rebinding is qualitatively determined by the appearance of a $\nu_{Fe-His} \simeq 222$ cm^{-1} at long times (>1 ms). Under our experimental conditions, such a band can only result from the photolysis of heme a_3 sites that have rebound CO. The net effect of ligand rebinding is to continuously upshift the frequency of ν_{Fe-His}. As shown in Figure 5 this behavior produces the predicted line broadening of the two-state model as described above and thus offers a counterpart to the continuous relaxation of the proximal hemepocket. Indeed, as the 222-cm^{-1} component becomes dominant (at $\Delta t \geq 10$ ns) the contribution from the remaining unbound equilibrium sites becomes apparent as a distinct low-frequency shoulder which decreases in intensity with time.

The kinetics of CO rebinding in cytochrome oxidase are considerably slower than those of Hb. Indeed at the CO solution concentrations (~1 mM) used in this study, the ligand rebinding rate is not appreciability faster than that predicted by previously measured second-order (nongeminate) rate constants (1–10 ms).[37] These data point to dramatic differences in the distal pockets of oxidase and hemoglobin. The suppression of CO geminate recombination must arise from either (1) the escape of nearly all photolyzed ligands from the pocket or (2) an alternate CO binding site within the pocket. The efficiency of ligand escape from the hemepocket is predicted upon the relative activation barriers to rebinding vs. escape and/or the diffusivity of the ligand through the protein.

The rate of ligand rebinding would be expected to be quite sensitive to the activation barrier encountered at the heme. This barrier should be significantly modulated by the proximal hemepocket geometry. The relaxation of the proximal hemepocket of cytochrome a_3 is, as discussed above, a relatively slow process. Thus, especially during the first 300 ns after photolysis, the heme–protein geometry strongly resembles that of the ligand-bound species. According to transition-state theory,[39] this situation should facilitate the rebinding of the dissociated CO by lowering the activation barrier of this process. Similar arguments have been used to explain the differences in geminate recombination and overall affinity between T-state (fast relaxing) and R-state (slow relaxing) hemoglobins.[4-10] It is apparent that the dynamics of the heme a_3 proximal pocket is not a viable explanation for the observed ligand rebinding behavior and that distal pocket effects play a dominant role in the lack of geminate recombination.

Previous spectroscopic studies have established large structural differences between the distal pockets of cytochrome a_3 and Hb. Resonance Raman studies of equilibrium cytochrome a_3·CO by Rousseau and co-workers[32] have determined that the Fe–C–O group in cytochrome a_3·CO is linear but tilted from the normal to the heme plane and that little or no heterogeneity exists in the heme–ligand geometry. Similar conclusions were reached in an infrared study of low-temperature cytochrome a_3·CO by Fiamingo et al.[25] where the narrow line widths of the C=O stretching vibration were interpreted as indicating a highly ordered, nonpolar carbon monoxide environment. That same study conclusively demonstrated that, in the low-temperature species, the Cu_B center provided a readily accessible second binding site for CO which had been photolyzed from the heme a_3. Fits to the observed power law dependence of CO rebinding to heme a_3 yield an enthalpy and entropy of activation for Cu_B·CO,$Fe_{a3}^{2+} \rightarrow Cu_B$, Fe_{a3}^{2+}·CO of ~40 kJ/mol and −77 J/(mol·K), respectively. Similar values for the activation enthalpy of CO rebinding were obtained from cryogenic absorption studies conducted by Sharrock and Yonetani.[24] HbA·CO, on the other hand, has been determined by crystallography to possesses an Fe–C bond that is perpendicular to the heme plane and a bent Fe–C–O geometry. An extensive series of low-temperature transient absorption studies of HbCO photolysis by Frauenfelder and co-workers[3] has characterized the activation enthalpy for recombination to be ≤10 kJ/mol.

Our room temperature results are consistent with a large barrier to ligand rebinding to heme a_3. It is difficult to assess whether ligand removal from the pocket occurs via escape into the surrounding solvent or binding to the Cu_B. Extrapolation of the activation energies calculated by Fiamingo et al.[25] to room temperature results in a rate constant of ~10^2 s^{-1}, whereas the pseudo-first-order rate constant for binding of ligand from the bulk solvent yields a rate of ~70 s^{-1}.[40] Thus, both phenomena would be predicted to result in ligand rebinding on the observed ~10 ms time scale. The dependence of ligand rebinding rate upon CO concentration in the bulk solvent (see Figure 3) implicates solvated CO molecules in the rebinding process. This does not preclude the participation of Cu_B in the ligation kinetics but it would appear to rule out the direct rebinding by the heme of geminate CO from the Cu_B·CO site as the rate-limiting kinetic step at room temperature.

Conclusions

This study has demonstrated that while some similarities exist between the photolytic transient species of hemoglobin and cytochrome a_3, the response of the heme a_3 pocket is distinctive in a number of ways: (a) the correlation between Fe–His bond strength and the frequency of ν_4 observed in a wide variety of Hb transients is apparently absent in cytochrome a_3 transients, (b) geminate CO recombination is apparently absent for cytochrome a_3, and (c) the kinetics of a_3 hemepocket relaxation are biphasic with virtually no change in the frequency of ν_{Fe-His} during the first 200 ns subsequent to photolysis. Cytochrome a_3 evidently possesses a more open distal pocket than Hb which significantly reduces geminate CO recombination. Cu_B may play a role in ligand rebinding, but our room temperature data offer no evidence for a rate-determining step involving CO binding to Cu_B. Analysis of the line width of ν_{Fe-His} during a_3 proximal hemepocket relaxation subsequent to ligand photolysis reveals the cytochrome a_3 pocket evolves in a continuous, visoelastic manner rather than through a two-state step-function-type mechanism. The lack of significant proximal hemepocket evolution during the first ~300 ns after photolysis strongly suggests that at least two kinetic processes are operative within the protein, the first involving protein conformational changes distant from the heme and the second producing the observed relaxation of ν_{Fe-His} to its equilibrium frequency.

Acknowledgment. This work was performed at the University of New Mexico and was supported by the National Institutes of Health (GM33330 to M.R.O. and GM25480 to G.T.B.).